^{111}In-DOTA-Lanreotide Scintigraphy in Patients with Tumors of the Lung

Tatjana Traub, Ventzislav Petkov, Sedat Ofluoglu, Thomas Pangerl, Markus Raderer, Barbara J. Fueger, Wolfgang Schima, Amir Kurtaran, Robert Dudczak, and Irene Virgolini

Departments of Nuclear Medicine, Pulmonology, Oncology, and Radiology and Ludwig Boltzmann Institute of Nuclear Medicine, University of Vienna, Vienna; and Nuclear Medicine Institute, Hospital Lainz, Vienna, Austria

Imaging with radiolabeled somatostatin (SST) analogs has recently been established for the localization of various human SST receptor (hsstr)-positive tumors, including neuroendocrine tumors, lymphomas, and non–small cell lung cancer (NSCLC). **Methods:** ^{111}In-1,4,7,10-tetraazacyclododecane-*N*,*N*′,*N*″,*N*‴-tetraacetic acid-lanreotide (DOTA-LAN) scintigraphy (150 MBq; 7 nmol per patient) was performed on 47 patients (28 patients with primary tumors, 19 patients with lung metastases from other tumors) to evaluate the tumor binding in patients with histologically confirmed lung cancer. A group of 27 tumor patients without documented lung lesions served as the control group. Early and delayed planar and SPECT images were acquired. Whole-body scintigraphy was performed at 0.5, 4–6, 24, and 48 h after injection for tumor dose estimation. In addition, hsstr subtype expression and radioligand binding characteristics were studied in vitro using lung tumor samples (n = 15). **Results:** ^{111}In-DOTA-LAN indicated the primary lung tumor in 16 of 16 NSCLC patients. Lymph node metastases were visualized in 6 of 6 NSCLC patients, and bone metastases were seen in 3 of 3 NSCLC patients. ^{111}In-DOTA-LAN scintigraphy indicated lung carcinoid in 5 of 5 patients and small cell lung cancer lesions in 6 of 6 patients. Multiple lung metastases were shown in all 6 patients with non-Hodgkin's lymphoma and in the 1 patient with Hodgkin's disease, 5 of 5 colorectal adenocarcinoma patients, 4 of 4 carcinoid patients, 2 of 2 neuroendocrine carcinoma (NEC) patients, and 1 of 1 angiosarcoma patient. Pulmonary tumor sites not indicated by CT or MRI were visualized in 6 of 47 tumor patients (i.e., 13%; lung metastases in 1 carcinoid patient and 1 NEC patient, lymph node metastases in 1 carcinoid patient and 2 NSCLC patients, bone metastases in 1 carcinoid patient). The estimated lung tumor dose ranged between 0.2 and 5 mGy/MBq. Focal lung uptake of ^{111}In-DOTA-LAN was not observed in any of the 27 control patients. In vitro binding studies indicated high-affinity binding sites for ^{111}In-DOTA-LAN in NSCLC samples (dissociation constants, 0.5 and 4 nmol/L) with predominant expression of hsstr4. **Conclusion:** ^{111}In-DOTA-LAN yields high tumor binding for various human lung tumors. Consecutively, radiopeptide therapy may offer a potential new treatment alternative for some lung tumor patients.

Key Words: somatostatin; receptor imaging; lanreotide; lung cancer

J Nucl Med 2001; 42:1309–1315

One of the most frequent malignancies worldwide is lung cancer. Invasive methods such as bronchoscopy, including bronchial washing and brushing, have a limited sensitivity of 65% for malignancy and adding transbronchial biopsy increases the sensitivity to 79% (*1*). Percutaneous CT-guided fine-needle biopsy has a sensitivity and a specificity of approximately 95% but may be associated with morbidity such as bleeding or perforation (*2*). However, noninvasive methods, including conventional radiologic methods (i.e., CT, radiography), may show inconclusive results in a significant number of cases. A 75%–85% specificity for malignant pulmonary nodules has been reported with conventional contrast-enhanced CT (*3*). Recently, Lowe et al. (*4*) reported a sensitivity of 92% and a specificity of 90% for ^{18}F-FDG PET. Although early detection and treatment may lead to improved survival, approximately 70% of lung cancers are inoperable at diagnosis, and chemotherapy and external radiation therapy are of palliative but, nevertheless, limited value (*5*).

Successful imaging of small cell lung cancer (SCLC) and non–small cell lung cancer (NSCLC) has been shown with somatostatin (SST) analogs, such as ^{111}In-diethylenetriaminepentaacetic acid (DTPA)-D-Phe^1-octreotide (OCT (*6,7*)) or ^{99m}Tc-P829 (*8*). These tracers bind to human SST receptors (hsstr) expressed on the surface of tumor cells. So far, 5 different hsstr subtypes have been been cloned and characterized in detail (*9–16*). We have recently shown that 1,4,7,10-tetraazacyclododecane-*N*,*N*′,*N*″,*N*‴-tetraacetic acid-lanreotide (DOTA-LAN) apparently targets hsstr2 through hsstr5 with high affinity (i.e., dissociation constant [K_d], approximately 1–10 nmol/L) and hsstr1 with lower affinity (K_d, approximately 200 nmol/L) (*17*); clinical data have indicated a high tumor accumulation (i.e., 0.4–5 mGy/MBq) of ^{111}In-DOTA-LAN in various tumor types (*18*).

In this study we have evaluated prospectively the tumor binding of ^{111}In-DOTA-LAN in patients with primary malignancies of the lung or secondary tumoral deposits (or both) in vitro and in vivo.

MATERIALS AND METHODS

Patients

The study group (Table 1) consisted of 28 patients with histologically verified primary lung tumors, including 16 patients with

Received Nov. 22, 2000; revision accepted May 14, 2001.

For correspondence or reprints contact: Tatjana Traub, MD, Department of Nuclear Medicine, University of Vienna, Waehringer Guertel 18-20, 1090 Vienna, Austria.

NSCLC (6 patients with squamous cell carcinoma, 10 with adenocarcinoma), 6 patients with SCLC, and 6 patients with carcinoid tumors. Furthermore, 19 patients had lung metastases from other primary tumors, such as lymphoma in 7 patients (non-Hodgkin's lymphoma in 6, Hodgkin's disease in 1), gut carcinoid in 4 patients, rectal adenocarcinoma in 5 patients, angiosarcoma in 1 patient, and neuroendocrine carcinoma (NEC) in 2 patients. Twenty-seven patients without lung metastases served as controls, including 8 patients with intestinal adenocarcinoma, 6 patients with nonmedullary thyroid cancer, 4 patients with lymphoma, 8 patients with intestinal carcinoid, and 1 patient with pheochromocytoma. The application of ^{111}In-DOTA-LAN to patients was approved by the ethical committee of the medical faculty of the University of Vienna. All patients gave written informed consent to participate. The study was performed according to the Declaration of Helsinki.

^{111}In-DOTA-LAN Preparation and Labeling

DOTA-LAN was synthesized in a 3-step reaction and labeled as described (*18,19*) using the peptide LAN (D-βNal-Cys-Tyr-D-Trp-Lys-Val-Cys-Thr-NH_2) and DOTA as starting materials. Briefly, after conjugation, the product, [DOTA-(D)-Nal^1]-LAN, was purified on a C_{18} reverse-phase, high-performance liquid chromatography (HPLC) column (Waters Corp., Milford, MA) using a water/acetonitrile/0.1% trifluoroacetic acid solvent system. A second HPLC purification using a water/acetonitrile/1% acetic acid solvent system yielded the pure compound as an acetate salt (purity, 97% [RP_{18}-HPLC]; mass spectrometry: found 1,504 MNa^+ by fast atom bombardment). Radiolabeling of DOTA-LAN was done with $^{111}InCl_3$ (no carrier added, >1,850 MBq/mL in 0.05 mol/L HCl; Nordion, Ontario, Canada). Quality control of the radiolabeled conjugate was performed with instant thin-layer chromatography using a mobile phase of 4 mmol/L ethylenediaminetetraacetic acid (EDTA) at pH 4.0. The peptide-bound activity remained at the origin and the previously uncomplexed radiometal moved with the solvent front as an EDTA complex. Formulation of the radiolabeled peptide in 0.075 mol/L NaCl, 0.05 mol/L NH_4OAc, 0.2 mol/L ascorbic acid, and 0.1% human serum albumin was performed before sterilization by filtration through a sterile Millex GV 0.2-mm membrane (Millipore, Milford, MA). A specific activity of about 20 MBq/nmol was achieved for ^{111}In-DOTA-LAN.

TABLE 1
Patient Characteristics

Characteristics	Number or size
No. of patients	47
Median age (y)	57 (Range, 22–70)
No. of patients with primary lung carcinoma	28
NSCLC	16
SCLC	6
Carcinoid	6
Diameter of lung lesions (cm)	Range, 0.7–4
No. of patients with lung metastases from other tumors	19
Lymphoma	7
Gut carcinoid	4
Colorectal adenocarcinoma	5
Neuroendocrine carcinoma	2
Angiosarcoma	1
Diameter of lung lesions (cm)	Range, 1–5

Gamma-Camera Imaging and Data Analysis

Planar and SPECT acquisitions were performed with a PRISM 1000 gamma camera equipped with a medium-energy collimator (Picker International, Cleveland Heights, OH). ^{111}In-DOTA-LAN was administered as a single intravenous bolus injection (150 MBq; 7 nmol DOTA-LAN per patient). The radiation of both energy peaks (173 and 247 keV) with a setting of windows at 20% was used. Serial whole-body acquisitions were recorded in anterior and posterior views (256 × 1024 matrix; 15 min each) at 0.5, 3–6, 24, and 48 h after injection. SPECT (128 × 128 matrix) and planar acquisitions (256 × 256 matrix; 500 kilocounts) were usually performed after the 3- to 6-h or 24-h (or both) whole-body scan. SPECT-imaging was performed in a 360° circle in 6° steps, 40–50 s per step. Ramp-filtered backprojection and 3-dimensional low-pass postfiltering were used. All scans were reconstructed in 3 projections at a slice thickness of 7 mm. Gamma-camera data were stored on disks. Data were processed by standard techniques using the dedicated computer software of the gamma camera with which the images were acquired.

Tissue samples obtained by transthoracic needle biopsy or surgery specimens were used as the gold standard for evaluating the accuracy (agreement) of ^{111}In-DOTA-LAN images in the diagnosis of lung lesions as benign or malignant in the case of single lesions. In the case of multiple tumors, only 1 representative had to be subjected to biopsy before imaging. The analysis of efficacy was based on blind evaluation of the ^{111}In-DOTA-LAN images. At least 2 nuclear medicine physicians independently evaluated the images of each patient without any knowledge of the patient's demographic or background characteristics, medical history, clinical presentation, or results of other diagnostic tests (i.e., chest radiography, contrast-enhanced CT, biopsy, FDG PET). ^{111}In-DOTA-LAN images were evaluated for the presence or absence of uptake in the right lung, left lung, mediastinum, and hilar area. In addition, other areas of increased uptake were recorded. After assessment of the scans, results were correlated with CT images that were no older than 6 wk.

For dosimetric calculations, regions of interest (ROIs) were drawn on whole-body scintigrams at each given time point. The mean of anterior and posterior counts was calculated for large ROIs of the lung, liver, spleen, kidneys, and urinary bladder. In addition, ROIs were drawn for all tracer accumulations regarded as tumor sites in the lungs and in all other regions of the body and background regions using the software written for the Picker analyzing system. Analysis of the gamma-camera data was done with correction for background and decay from the time of injection. Mono- and biexponential time–activity curves were fitted. The residence times were determined using these data and the respective half-lives of ^{111}In. The derived residence times were used for organ dose calculations on the basis of the Medical Internal Radiation Dose concept (*20*). Absorbed organ dose was calculated by applying the MIRDOSE 3 software (*21*). For assessment of lung tumor doses, the "nodule module" option of the program for estimating the S values of spheric tumors was applied. The effective dose, as defined by the International Commission on Radiological Protection, was also calculated (*22*).

In Vitro hsstr Evaluation (Northern Analysis)

For investigation of hsstr expression, snap-frozen tumor specimens from patients with NSCLC and carcinoids were put into liquid nitrogen. Total RNA from the homogenate was extracted following the Trizol (Invitrogen Corp., Carlsbad, CA) extraction

protocol, a modification of the RNA extraction procedure described by Chromczynski and Sacchi (*23*). The integrity of RNA was confirmed by agarose gel electrophoresis and staining with ethidium bromide. Northern blot analysis of hsstr was performed as reported (*24*). Briefly, Northern transfer of 10–20 μg total RNA was done using Nytran membranes (Schleicher & Schleicher, Vienna, Austria) by capillary blotting overnight after fixation of RNA to the membranes by ultraviolet cross-linking. Specific probes for Northern hybridization were generated by restriction cutting of the plasmids carrying the probes with the appropriate restriction enzymes followed by separation on an agarose gel. The probes were then purified with the Qiaex gel purification kit (Qiagen, Santa Clarita, CA) and labeled with the Redivue random prime labeling kit (Amersham, Buckinghamshire, U.K.) and [^{32}P]deoxycytidine triphosphate (Amersham). Hybridization was performed as described (*24*). Four hours after hybridization of the membranes at 42°C in a hybridization solution containing 50% formamide, 5× Denhardt's solution, 5× sodium chloride/sodium citrate (SSC), 0.2% sodium dodecyl sulfate (SDS), and 100 μg/mL salmon sperm DNA, the labeled product was added in fresh hybridization buffer. Hybridization was performed overnight. Thereafter, blots were rinsed twice at room temperature with 2× SSC buffer containing 0.1% SDS and exposed to an x-ray film (Hyperfilm; Amersham). The results of hsstr subtype expression were obtained by laser densitometric measurements, with higher numeric values corresponding to higher signal intensity on x-ray films using GelScan XL software (Pharmacia, Upsala, Sweden). COS7 cells, nontransfected and transfected with the respective hsstr subtype-specific plasmids, were used as controls.

Radioligand Binding Assays

Radioligand binding studies were performed for evaluation of DOTA-LAN binding sites expressed on tumor tissues. The assay conditions were similar to those reported for other peptide ligands (*25,26*). Tissues were cut into pieces and homogenized by means of a tissue homogenizer in ice-cold Tris-HCl buffer at pH 7.4. For each reaction vial, 30–50 μg membrane protein were used. The saturation experiments were performed in triplicate under steady-state conditions at 4°C. Membrane fractions were incubated with increasing concentrations of ^{111}In-DOTA-LAN (0.01–10 nmol/L) in the absence (total binding) or the presence of DOTA-LAN and SST-14 (1 μmol/L, nonspecific binding) for 90 min. Specific binding was determined as the difference between total and nonspecific binding. Binding data were analyzed according to Scatchard (*27*). The number of binding sites (binding capacity [B_{max}]) and the binding affinity (K_d, concentration of labeled ligand causing half-maximal binding) were determined. For displacement studies, tumor cell membranes were incubated with 0.1 nmol/L ^{111}In-DOTA-LAN in the absence (total binding) and the presence of increasing concentrations (0.1 nmol/L to 1 μmol/L, nonspecific binding) of DOTA-LAN for 90 min. For separation of bound from free ligand, the reaction product was diluted after incubation 1:10 with assay buffer and rapidly filtered through GF/c filters (Whatman, Inc., Clifton, NY). The radioactivity of each resulting pellet was counted in a γ-counter for 1 min each. The concentrations of unlabeled ligand causing half-maximal inhibition were determined from the resulting displacement curves.

RESULTS

^{111}In-DOTA-LAN Scintigraphy

^{111}In-DOTA-LAN scintigraphy identified lung tumor lesions ranging between 0.7 and 5 cm in diameter in all 47 patients with histologically verified lung tumors (Fig. 1). Table 2 compares the ^{111}In-DOTA-LAN results with the CT results in 28 patients with primary lung tumors. ^{111}In-DOTA-LAN was able to visualize the primary tumor lesion in all 16 patients with NSCLC and in all 6 patients with SCLC. Lymph node metastases were identified in 6 of 6 patients with NSCLC and in 4 of 4 patients with SCLC. In 2 NSCLC patients (abdominal lymph node neoplasia [LNN] in 1 patient, mediastinal LNN in the other patient) and in 1 lung carcinoid patient, additional lymph node involvement was detected by ^{111}In-DOTA-LAN, which was also confirmed by FDG PET but not indicated by CT at that time. Documented liver metastases were present in 5 patients

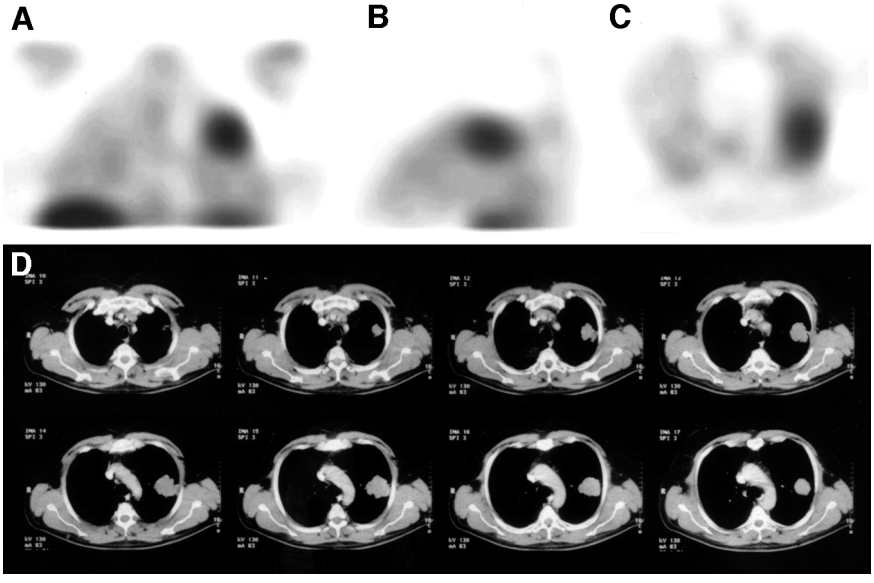

FIGURE 1. Coronal (A), sagittal (B), and axial (C) views of ^{111}In-DOTA-LAN SPECT study of patient with squamous cell carcinoma of left lung. (D) Corresponding CT study.

TABLE 2
Positive Results of ^{111}In-DOTA-LAN Compared with CT and Bone Scintigraphy

Histology	No. of patients	Primary	LNN (1–3 cm)	Liver	Bone
NSCLC	16	16/16	6*/6	0/1	0/3
Adenocarcinoma	10	10/10	3/3	0/1	0/1
SCC	6	6/6	3/3		0/2
SCLC	6	6/6	3/4	1/2	2/2
Carcinoids	6	6/6	1*/1	2/2	1/0

*Additional lymph node metastases were found in 2 patients with NSCLC and in 1 patient with carcinoid, and additional liver lesion was found in 1 carcinoid patient.

LNN = lymph node neoplasia; SCC = squamous cell carcinoma.

TABLE 3
Organ and Tumor Dose Estimates (mGy/MBq) for ^{111}In-DOTA-LAN

Organ	Median	Range
Gonads	0.06	0.05–0.11
Kidneys	0.33	0.24–0.46
Liver	0.15	0.11–0.25
Lung	0.07	0.06–0.48
Red marrow	0.07	0.06–0.11
Spleen	0.34	0.26–0.64
Urinary bladder	0.18	0.16–0.25
Effective dose (mSv/MBq)	0.10	0.09–0.12
Lung primary	1.30	0.20–5.00
Lung metastases	0.49	0.26–1.60

(1 NSCLC patient, 2 SCLC patients, 2 carcinoid patients) and were visualized in 1 SCLC patient and 2 carcinoid patients. Bone metastases documented in 5 patients (3 NSCLC patients, 2 SCLC patients) were seen in both patients with SCLC.

In all 7 lymphoma patients, the 4 patients with gut carcinoids, the 5 colorectal adenocarcinoma patients, and the 1 NEC patient, ^{111}In-DOTA-LAN scintigraphy detected lung metastases as also seen on CT. Moreover, this tracer detected lung metastases that were not documented previously by CT of another NEC patient who was imaged by additional ^{111}In-OCT scintigraphy. In the patient suffering from angiosarcoma, metastases known in lung, mediastinal lymph nodes, liver, and bone were visualized by ^{111}In-DOTA-LAN.

All lesions were identified by ^{111}In-DOTA-LAN in the cohort of 19 tumor patients with secondary spread to the lung, but focal accumulations of ^{111}In-DOTA-LAN indicating liver metastases were also present in 2 of these patients. In addition, LNN metastases were seen in 2 of 3 patients.

Radiation Dose Estimates for ^{111}In-DOTA-LAN

After fitting individual ROIs over organs and primary tumors or metastases, radiation absorbed doses were calculated for the spleen (median, 0.34 mGy/MBq), the kidneys (median, 0.33 mGy/MBq), the urinary bladder (median, 0.18 mGy/MBq), the liver (median, 0.15 mGy/MBq), the lung (median, 0.07 mGy/MBq), the bone marrow (median, 0.07 mGy/MBq), and the gonads (median, 0.06 mGy/MBq). The effective dose ranged between 0.09 and 0.12 mSv/MBq (median, 0.10 mSv/MBq). After evaluating the mean residence time, τ, the median radiation dose to the lung tumors or metastases was 1.3 mGy/MBq (range, 0.2–5 mGy/MBq) (Table 3).

hsstr Expression

The presence of hsstr subtype-specific messenger RNA (mRNA) in NSCLC was analyzed by Northern blot analysis (Table 4). Strong expression of hsstr4 was found in all 4 squamous cell carcinoma samples, and hsstr2 was expressed in 2 of these specimens. hsstr2 expression was found in both adenocarcinomas investigated, whereas hsstr4 was expressed in only 1. The highest signal intensity on Northern blotting was found for hsstr4 in squamous cell carcinomas (Fig. 2). hsstr2 through hsstr4 were expressed in both lung carcinoids and in the 2 SCLC tissue samples. hsstr5 was expressed in carcinoids but not in SCLC tissue samples.

Radioligand Binding Results

^{111}In-DOTA-LAN receptor binding assays performed with NSCLC tissue samples (Fig. 3) obtained from scintigraphically evaluated NSCLC patients ($n = 2$) indicated an abundant number of hsstr binding sites. By Scatchard analysis, 2 distinct high-affinity binding classes were detected: 1 with a B_{max1} of 0.30 pmol/mg protein (K_d, 4 nmol/L) and the other with a B_{max2} of 0.05 pmol/mg protein (K_d, 0.5 nmol/L).

DISCUSSION

The high-level expression of hsstr on various tumor cells compared with normal tissues or blood cells has provided the molecular basis for successful application of radiola-

TABLE 4
Northern Blot Analysis of mRNA Expression of SST Receptor (hsstr) Subtypes 1–5

Patient no.	Histology	hsstr1	hsstr2	hsstr3	hsstr4	hsstr5
1	SCC	−	+	−	++	+
2	SCC	−	++	+	+++	+
3	SCC	−	++	+	+++	+
4	SCC	−	+	−	++	+
5	A	−	+	−	+	−
6	A	−	+	−	−	−
7	C	+	+	++	++	++
8	C	−	+	++	++	++
9	SCLC	−	++	++	++	−
10	SCLC	−	++	−	++	−

SCC = squamous cell carcinoma; − = negative; + = weak expression; ++ = intermediate expression; +++ = strong expression; A = adenocarcinoma; C = carcinoid.

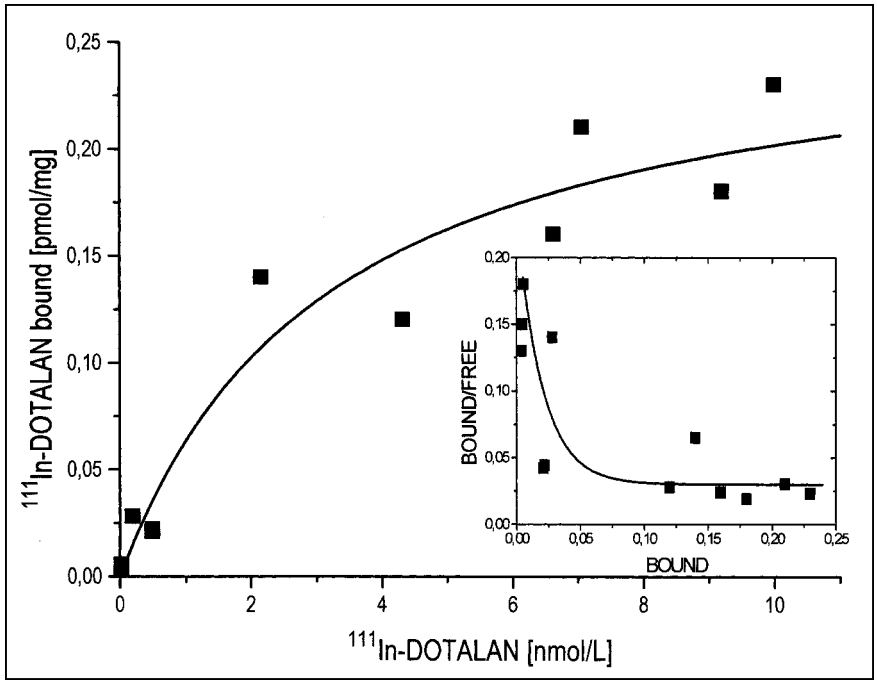

FIGURE 2. ^{111}In-DOTA-LAN specific binding to squamous cell carcinoma. Inset shows 2 high-affinity binding classes: K_d values of 0.5 and 5 nmol/L.

beled SST analogs for receptor-targeted diagnosis and treatment (*6*,*26*,*28*,*29*). Our study was performed to investigate the clinical potential of ^{111}In-DOTA-LAN for tumor localization. ^{111}In-DOTA-LAN visualized the primary tumor in all 28 patients and lung metastases in all 19 patients included in the series. Mediastinal lymph node metastases were also revealed in all patients except 1 patient with SCLC; this omission was probably associated with the small size of the lesion (7 mm in diameter as revealed on CT).

Apart from lesions already revealed by conventional imaging, additional lesions were detected in 5 of the 47 patients with lung tumors. A priori unknown lymph node metastases were visualized in 2 patients with adenocarcinomas and in 1 SCLC patient, whereas liver metastases and additional lung lesions were seen in 1 carcinoid patient. Moreover, ^{111}In-DOTA-LAN scintigraphy was the first imaging technique to give a positive result in 1 of the 2 patients with neuroendocrine tumors. These results indicate that ^{111}In-DOTA-LAN scintigraphy may provide new or additional information (or both) in the staging of lung tumors, including NSCLC. Our results with ^{111}In-DOTA-LAN are in line with data obtained with ^{111}In-DTPA-D-Phe^1-OCT (*6*,*30*), which has consistently displayed a high diagnostic value in patients with carcinoids.

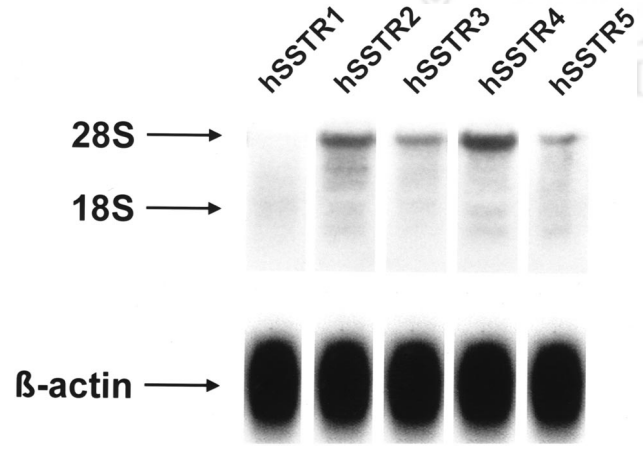

FIGURE 3. Northern blot analysis (patient 3, Table 4). Transfected and nontransfected COS7 cells were used as positive and negative controls, respectively.

The possibility of false-positive SSTR scintigraphic results in patients with granulomatous disease has already been reported (*7*,*8*). In 1 of our NSCLC patients we also observed an ^{111}In-DOTA-LAN–positive lesion that was confirmed as tuberculosis by biopsy, indicating binding of DOTA-LAN to intralesional inflammatory cells. However, previous studies have shown (*6*,*7*,*18*,*29*,*31*) that the binding of SST analogs to tumor lesions is more avid than in granulomatous and other nonmalignant processes. Blum et al. (*8*) have described the correct identification or exclusion of malignancy in 27 of 30 subjects with radiographically indeterminate solitary pulmonary nodules investigated with the ^{99m}Tc-labeled SST analog P829, with a favorable sensitivity of 93% and a specificity of 88% compared with transthoracic needle biopsy. These data appear to be superior to those of FDG PET, which has been reported to be more accurate in revealing intrathoracal metastatic disease compared with CT or MRI (*32*,*33*). However, these data have to be interpreted with caution because larger studies are still warranted to identify the specificity of SST-based tracers in terms of distinction between benign from malignant tissues.

From the clinical point of view, clear-cut exclusion of malignancy by means of scintigraphy appears not to be possible to date. Nonetheless, a positive scan result should certainly lead to invasive techniques to verify or to rule out malignancy by histologic investigation.

In vitro studies have shown that up to 70% of SCLC express specific binding sites for hsstr (*34*), whereas the absence and presence of hsstr expression have been reported in NSCLC (*25*,*35*,*36*). Furthermore, uptake of radiolabeled SSTR ligands by nonmalignant cells within the tumor (stroma, inflammatory cells, necrotic tissue, vessels) has been debated (*37*,*38*). To our knowledge, this is the first report on hsstr4 and hsstr5 expression in NSCLC tissues. Thomas et al. (*35*) described hsstr1 and hsstr2 gene expression but no hsstr3 gene expression using a polymerase chain reaction technique, and the transcription level was higher for hsstr1 than for hsstr2. However, 37% of all polymerase chain reactions were negative. O'Byrne et al. (*36*) found a single class of specific high-affinity binding sites in 3 of 3 NSCLC tissues (K_d, 8.1–6 nmol/L; B_{max}, 0.9–1.9 pmol/mg), leading the authors to hypothesize that NSCLC cells per se do not express specific binding sites and that binding might be caused by interaction with other cells such as stroma cells, inflammatory cells, or necrotic tissue. Sreedharan et al. (*37*) reported the expression of hsstr on human lymphocytes, suggesting that inflammatory reactions resulting in lymphocytic infiltration might lead to positive results. Another potential basis of positive results in terms of SSTR scintigraphy was presented by Reubi et al. (*38*): hsstr expression was found not only in tumoral tissues (especially in intestinal carcinomas) but also in the peripheral vascular system, suggesting a crucial regulatory role for hemodynamic tumor–host interactions. Furthermore, the failure to document hsstr expression in tumors by autoradiography could be associated with an insufficient sensitivity of this technique or absence of receptor expression caused by a low translation rate of mRNA, posttranslational modification, or a rapid turnover of surface receptors (*36*). We showed by Northern blot analysis that squamous cell carcinomas express mRNA for hsstr4 and hsstr5 and also, to a lesser extent, hsstr3 and hsstr2. Adenocarcinomas, which also express other hsstr subtypes, seem to have a different expression pattern. Earlier studies have also described different results for colorectal adenocarcinomas (*17*). Taken together, our results (an abundant number of binding sites, a high binding affinity for DOTA-LAN in NSCLC tissue, positive scan results in vivo) support the hypothesis of the presence of various hsstr subtypes in NSCLC.

Because of the demand of new therapeutic concepts for patients with inoperable cancer or tumors refractory to radiation and chemotherapy, we have also performed dosimetric calculations. Our data are comparable to previous results (*18*) on tumor dose estimates showing doses ranging from 0.2 to 5 mGy/MBq for ^{111}In-DOTA-LAN. In addition, calculations for projected doses of ^{90}Y-DOTA-LAN, which has a similar biodistribution and is assumed to display behavior identical to that of ^{111}In-DOTA-LAN in human tumors (*18*,*19*), ranged from 5 to 50 mGy/MBq. Preliminary encouraging data on successful treatment of hsstr-positive tumors with radiolabeled SST analogs have been reported, and DOTA-LAN may present a potential alternative approach (*18*,*39*).

CONCLUSION

On the basis of hsstr recognition, ^{111}In-DOTA-LAN yields a high diagnostic efficacy and promising tumor accumulation in terms of dosimetry in a large variety of human lung tumor types. The high tumor uptake for SST analogs might provide the basis for experimental therapy approaches in patients with lung cancer.

ACKNOWLEDGMENTS

The authors are indebted to the technologists of the department involved in the study acquisition procedures for their working effort and also thank Drs. Peter Angelberger, Christoph Brunner, Maria Leimer, Markus Peck-Radosvaljevic, Emilia Halvadijeva, and Yang Qiong for their constructive comments and organizational help. This study was supported in parts by the Austrian National Bank (Jubiläumsfondsprojects 7556 and 7841) and the Ludwig Boltzmann Institute of Nuclear Medicine.

REFERENCES

1. Salathe M, Bower JH, Bryan CL, et al. Transbronchial needle aspiration in routine fiberoptic bronchoscopy. *Respiration.* 1992;59:5–8.
2. Polak J, Kubik A. Percutaneous thin needle biopsy of malignant and nonmalignant thoracic lesions. *Radiol Diagn (Berl).* 1989;30:177–182.
3. Swensen S, Brown L, Colby T, et al. CT-evaluation of enhancement with iodinated contrast material. *Radiology.* 1995;194:393–398.
4. Lowe VJ, Fletcher JW, Gobar L, et al. Prospective investigation of positron emission tomography in lung nodules. *J Clin Oncol.* 1998;16:1075–1084.
5. Ginsberg R, Kris MG, Armstrong JG. Cancer of the lung. In: DeVita VT, Hellman S, Rosenberg SA, eds. *Cancer: Principles & Practice of Oncology*. 4th ed. Philadelphia, PA: JB Lippincott; 1993:637–758.
6. Krenning EP, Kwekkeboom DJ, Bakker W, et al. Somatostatin receptor scintigraphy with In-111-DTPA-D-Phe1 and I-131-Tyr-3-octreotide: the Rotterdam experience with more than 1000 patients. *Eur J Nucl Med.* 1993;20:716–731.
7. Kwekkeboom D, Krenning E, Bakker W, et al. Radioiodinated somatostatin analog scintigraphy in small-cell lung cancer. *J Nucl Med.* 1991;32:1845–1848.
8. Blum J, Handmaker H, Rinne N. The utility of a somatostatin-type receptor binding peptide radiopharmaceutical (P829) in the evaluation of solitary pulmonary nodules. *Chest.* 1999;115:224–232.
9. Yamada Y, Post SR, Wang K, et al. Cloning and functional characteristics of a family of human and mouse somatostatin receptors expressed in brain, gastrointestinal tract, and kidney. *Proc Natl Acad Sci USA.* 1992;89:251–255.
10. Yamada Y, Reisine S, Law SF, et al. Somatostatin receptors, an expanding gene family: cloning and functional characterization of human SSTR3, a protein coupled to adenylal cyclase. *Mol Endocrinol.* 1992;6:2136–2142.
11. Yamada Y, Kagimoto S, Kubota A, et al. Cloning, functional expression and pharmacological characterization of a fourth (hsstr4) and a fifth (hsstr5) human somatostatin receptor subtype. *Biochem Biophys Res Commun.* 1993;195:844–852.
12. Yasuda K, Res-Domiano S, Breder CA, et al. Cloning of a novel somatostatin receptor, SSTR3, coupled to adenylate cyclase. *J Biol Chem.* 1992;267:20422–20428.
13. Demchyschyn LL, Srikant CB, Sunahara RK, et al. Cloning and expression of a human somatostatin-14-selective receptor variant (somatostatin receptor 4) located on chromosome 20. *Mol Pharmocol.* 1993;43:894–901.
14. Bell GI, Yasada K, Kong H. Molecular biology of somatostatin receptors. *Ciba Found Symp.* 1995;190:65–88.

15. Corness JD, Demchyschyn LL, Seeman P. A human somatostatin receptor (SSTR3), located on a chromosome 22, displays preferential affinity for somatostatin-14 like peptides. *FEBS Lett.* 1993;321:279–284.
16. Rohrer L, Raulf F, Bruns C, et al. Cloning and characterization of a fourth human somatostatin receptor. *Proc Natl Acad Sci USA.* 1993;90:4196–4200.
17. Virgolini I, Pangerl T, Bischof C, et al. Somatostatin receptor subtype expression in human tissues: a prediction for diagnosis and treatment of cancer? *Eur J Clin Invest.* 1997;27:645–647.
18. Virgolini I, Szilvasi I, Kurtaran A, et al. Indium-111-DOTA-lanreotide: biodistribution, safety and tumor dose in patients evaluated by somatostatin receptor-mediated radiotherapy. *J Nucl Med.* 1998;39:1928–1936.
19. Smith-Jones P, Bischof C, Leimer M, et al. DOTA-lanreotide: a novel somatostatin analog for tumor diagnosis and therapy. *Endocrinology*. 1999;140:5136–5148.
20. Loevinger R, Budinger T, Warson E. *MIRD Primer for Absorbed Dose Calculations*. Reston, VA: Society of Nuclear Medicine; 1988.
21. Stabin MG. MIRDOSE: personal computer software for internal dose assessment in nuclear medicine. *J Nucl Med.* 1996;37:538–546.
22. Johansson L, Mattson S, Nosslin B, Svegborn SR. Effective dose from radiopharmaceuticals. *Eur J Nucl Med.* 1993;19:933–938.
23. Chromczynski P, Sacchi N. Single-step method of RNA isolation by acid guanidinium thiocyanate-phenol-chloroform extraction. *Anal Biochem.* 1987;162:156–159.
24. Sambrook J, Fritsch EF, Maniatis T. *Molecular Cloning: A Laboratory Manual.* 2nd ed. Cold Spring Harbor, NY: Cold Spring Harbor Laboratory Press; 1989:739–752.
25. Virgolini I, Leimer M, Handmaker H, et al. Somatostatin receptor subtype specificity and in vitro binding of a novel tumor tracer, Tc-99m-P829. *Cancer Res.* 1998;58:1850–1859.
26. Reubi JC, Maurer R, von Werder K, et al. Somatostatin receptors in human neuroendocrine tumors. *Cancer Res.* 1987;47:551–558.
27. Scatchard G. The attraction of proteins for small molecules and ions. *Ann NY Acad Sci.* 1949;51:660–672.
28. Virgolini I, Yang Q, Li S, et al. Cross-competition between vasoactive intestinal peptide and somatostatin for binding to tumor cell membrane receptors. *Cancer Res.* 1994;54:690–700.
29. Virgolini I, Raderer M, Kurtaran A, et al. Vasoactive intestinal peptide (VIP) receptor imaging for the localization of intestinal adenocarcinomas and endocrine tumors. *N Engl J Med.* 1994;33:1116–1121.
30. Raderer M, Kurtaran A, Leimer M, et al. Value of peptide receptor scintigraphy using ^{123}I-vasoactive intestinal peptide and ^{111}In-DTPH-D-Phe^{1}-octreotide in 194 carcinoid patients: Vienna University experience, 1993 to 1998. *J Clin Oncol.* 2000;18:1331–1336.
31. Lamberts SWJ, Bakker WH, Reubi JC, Krenning EP. Somatostatin receptor imaging in the localization of endocrine tumors. *N Engl J Med.* 1990;323:1246–1249.
32. Lowe V, Fletcher J, Gobar L, et al. Prospective investigation of positron emission tomography in lung nodules. *J Clin Oncol.* 1998;16:1075–1084.
33. Nettelbladt OS, Sundin AE, Valind SO, et al. Combined fluorine-18-FDG and carbon-11-methionine PET for diagnosis of tumors in lung and mediastinum. *J Nucl Med.* 1998;39:640–647.
34. Reubi JC, Waser B, Sheppard M, Macaulay Y. Somatostatin receptors are present in small-cell but not in non-small primary lung carcinomas: relationship to EGF-receptors. *Int J Cancer.* 1990;45:269–274.
35. Thomas F, Brambrilla E, Friedmann A. Transcription of somatostatin receptor subtype 1 and 2 genes in lung cancer. *Lung Cancer.* 1994;11:111–114.
36. O'Byrne KJ, Halmos G, Pinski J, et al. Somatostatin receptor expression in lung cancer. *Eur J Cancer.* 1994;30:1682–1687.
37. Sreedharan SP, Kodama KT, Peterson KE, Goetzl EJ. Distinct subjects of somatostatin receptors on cultured human lymphocytes. *J Biol Chem.* 1989;264:949–952.
38. Reubi JC, Horisberger U, Laissue J. High density of somatostatin receptors in veins surrounding human cancer tissue: role in tumor-host interaction? *Int J Cancer.* 1994;56:681–688.
39. Leimer M, Kurtaran A, Smith-Jones P, et al. Response to treatment with yttrium 90-DOTA-lanreotide of a patient with metastatic gastrinoma. *J Nucl Med.* 1998;39:2090–2093.